



# The low-temperature interaction of NH<sub>3</sub>/NO/NO<sub>2</sub> + O<sub>2</sub> with Fe-ZSM-5 + BaO/Al<sub>2</sub>O<sub>3</sub> and H-ZSM-5 + BaO/Al<sub>2</sub>O<sub>3</sub>: Influence of phase separation and relevance for the NH<sub>3</sub>-SCR chemistry



Tommaso Selleri, Isabella Nova, Enrico Tronconi \*

Dipartimento di Energia, Laboratorio di Catalisi e Processi Catalitici, Politecnico di Milano, Via La Masa 34, I-20156 Milano, Italy

## ARTICLE INFO

### Article history:

Received 1 November 2016

Received in revised form 5 January 2017

Accepted 12 January 2017

Available online 17 January 2017

### Keywords:

NO oxidation

Standard SCR mechanism

Fe-zeolite catalyst

Nitrates

Nitrites

Chemical trapping

## ABSTRACT

In an effort to elucidate mechanism and intermediates of Standard SCR over metal-zeolite catalysts, we apply Transient Response Methods (TRM) to identify the mediating species in the low-temperature (120 °C) interaction of NO<sub>2</sub> + O<sub>2</sub>, NO + O<sub>2</sub> and NO + NO<sub>2</sub> + O<sub>2</sub> (NO/NO<sub>2</sub> = 10/1 v/v) with a composite Fe-ZSM-5 (Fe = 1% w/w) + BaO/Al<sub>2</sub>O<sub>3</sub> system in different configurations (physical mixture versus double-bed), corresponding to different degrees of separation of the two component phases. The results clearly indicate for the first time that the strong interaction between the two system components, already demonstrated in previous work, survives their complete segregation, proceeds via the gas phase, and is mediated by stable gaseous NOx species. The nature of the NOx species trapped on the BaO phase is identified by TPD experiments: in line with previous data, they include primarily nitrates for NO<sub>2</sub> adsorption, and nitrites for NO + O<sub>2</sub> adsorption at short exposure times. A new, striking finding is that formation of nitrites on BaO upon exposure of Fe-ZSM-5 + BaO/Al<sub>2</sub>O<sub>3</sub> to NO + O<sub>2</sub>, which involves the oxidative activation of NO on Fe-sites, is fully equivalent to the formation of nitrites observed upon exposing only BaO/Al<sub>2</sub>O<sub>3</sub> to NO<sub>2</sub> in excess NO. This suggests that NO<sub>2</sub> (possibly in the form of N<sub>2</sub>O<sub>3</sub>) may play the role of mediating gas-phase species generated by the oxidative activation of NO on Fe centers. The reactivity with NH<sub>3</sub> of nitrites trapped on BaO is probed by Temperature Programmed Surface Reaction (NH<sub>3</sub>-TPSR) runs, which show rapid dinitrogen formation from low temperatures when Fe-ZSM-5 is not only mixed with, but also placed downstream from BaO/Al<sub>2</sub>O<sub>3</sub>, thus confirming the stability of the NOx intermediate formed on Fe-centers, and linking it to the Standard SCR reactivity. Finally, in order to study the role of the metal redox sites in the reactivity of nitrites stored on BaO with ammonia, we compare NH<sub>3</sub>-TPSR experiments over a Fe-ZSM-5 catalyst and over a parent H-ZSM-5 zeolite with a drastically reduced Fe content (Fe ≈ 0.02% w/w). Results show that nitrites on BaO react with NH<sub>3</sub> to dinitrogen equally well on Fe- and on H-ZSM-5, which questions the role of the metal sites and therefore of the oxidative activation of NH<sub>3</sub> in such a step.

The present data emphasize the bifunctional (redox + acid) nature of the NH<sub>3</sub>-SCR catalytic chemistry at low temperatures, and should be considered in the development of comprehensive mechanisms for the Standard SCR reaction over Fe-zeolite catalysts.

© 2017 Elsevier B.V. All rights reserved.

## 1. Introduction

Emissions regulations for both compression and spark-ignited internal combustion engines are becoming more stringent worldwide, as it is no longer possible to achieve the limits imposed by international legislation by just improving the combustion technology. For lean burn Diesel engines, in particular, the NH<sub>3</sub>/Urea-Selective Catalytic Reduction process (NH<sub>3</sub>/Urea-SCR)

has been successfully demonstrated at the commercial scale and currently represents the best available technology for NOx abatement. In NH<sub>3</sub>-SCR converters, excellent deNOx performances are attained over metal-promoted zeolite catalysts thanks to their high activity in two main reactions, namely the Standard SCR reaction (NO + O<sub>2</sub> + NH<sub>3</sub>) and the Fast SCR reaction (NO + NO<sub>2</sub> + NH<sub>3</sub>) [1].

The elucidation of the SCR catalytic mechanisms over state-of-the-art metal-exchanged zeolites has been a central research topic in recent years [1–16] but, particularly for what concerns the Standard SCR reaction, a comprehensive and satisfactory account is still lacking. In recent publications we have investigated the NO + O<sub>2</sub> adsorption on physical mixtures of metal (Fe and Cu) promoted zeo-

\* Corresponding author.

E-mail address: [enrico.tronconi@polimi.it](mailto:enrico.tronconi@polimi.it) (E. Tronconi).

lites and BaO/Al<sub>2</sub>O<sub>3</sub> [12–14], with the aim of providing new insight in the catalytic chemistry of the low-temperature Standard SCR. In these works, we succeeded in trapping onto the BaO/Al<sub>2</sub>O<sub>3</sub> phase unstable nitrites generated by the oxidative activation of NO on the metal-zeolite catalyst, and we speculated on the possible existence of a gas-phase pathway responsible for the observed interaction between the two physical mixture components. Nitrites storage on BaO was demonstrated in several ways, including: (i) their thermal decomposition to an equimolar mixture of NO and NO<sub>2</sub> during TPD, (ii) N<sub>2</sub> formation during their reaction with NH<sub>3</sub> at low temperature, (iii) ex-situ IR analysis of the BaO/Al<sub>2</sub>O<sub>3</sub> phase after unloading and separation from the mechanical mixture.

In the present work, we further investigate the interaction of NO<sub>x</sub> + O<sub>2</sub> with composite Fe-ZSM-5 + BaO/Al<sub>2</sub>O<sub>3</sub> systems on the basis of a completely new set of data, with the dual goal of clarifying whether such an interaction proceeds indeed via gas phase, and of identifying the involved mediating species. To this purpose, herein we analyze the effect of phase segregation on the synergy between the two component phases. In particular, we have focused on the following configurations: (i) mechanical mixture with the two phases in loose contact; (ii) sequential segregated beds, where the two components (positioned in different orders) are separated by an inert quartz wool layer; (iii) single constituents of the mixture, individually tested.

The pathway leading to the trapping of nitrites on BaO is clearly relevant for the NO activation step in the Standard SCR chemistry, as discussed in the following paragraphs. To complete the analysis of the Standard SCR mechanism, herein we also investigate the subsequent reactivity of nitrites with NH<sub>3</sub>, and perform dedicated experiments on H-ZSM-5 to clarify the role of redox Fe centers in this second stage of the mechanism.

Altogether, the present experimental results are significant for the elucidation of the Standard SCR reaction chemistry over Fe-promoted zeolites, provide new elements for the development of a comprehensive SCR mechanism, and may be useful to discriminate rival mechanistic proposals.

## 2. Experimental

In this study, different systems comprising a Fe-ZSM-5 zeolite (22 mg), an H-ZSM-5 zeolite (22 mg) and in-house prepared BaO/Al<sub>2</sub>O<sub>3</sub> (44 mg), all in form of powders, were tested in different spatial arrangements. The Fe-ZSM-5 was a commercial catalyst manufactured by Zeolyst (CP 7117), with a SiO<sub>2</sub>/Al<sub>2</sub>O<sub>3</sub> ratio of 24, surface area of 300 m<sup>2</sup>/g and 1% w/w Fe content. The H-ZSM-5 sample was a commercial material manufactured by Zeolyst (CBV 2314), with a SiO<sub>2</sub>/Al<sub>2</sub>O<sub>3</sub> ratio of 23, surface area of 425 m<sup>2</sup>/g and 0.05% w/w Na<sub>2</sub>O content. ICP-MS analysis revealed a residual Fe content of 0.0235% w/w, i.e. significantly lower (over 40 times) with respect to the Fe-exchanged catalyst. Both zeolite powders were dried at 120 °C for 1 h and sieved to 120–140 mesh (average particle size = 115 µm). The BaO/Al<sub>2</sub>O<sub>3</sub> component (Ba content = 16% w/w) was prepared in-house by incipient wetness impregnation, using aqueous solutions of Ba(CH<sub>3</sub>COO)<sub>2</sub> (Sigma Aldrich, 99% pure) to impregnate the γ-alumina support (Versal 250 from Eurosupport: surface area = 200 m<sup>2</sup>/g and pore volume = 1.2 cm<sup>3</sup>/g) calcined at 800 °C. After impregnation, the powder was dried at 80 °C overnight, calcined at 500 °C for 5 h, and sieved to 140–200 mesh (average particle size = 90 µm). Cordierite with 120–140 mesh size was added for dilution. In all runs, the powders were loaded in a quartz microflow reactor (ID = 7 mm). The following configurations have been tested: (i) a physical mixture of Fe-ZSM-5 and BaO/Al<sub>2</sub>O<sub>3</sub> powders (identified in the following as Fe-Ba-MM) with the two phases in loose contact and a total dilution with cordierite up to 120 mg; (ii) a double-bed configuration with Fe-ZSM-5 first,

followed by a BaO/Al<sub>2</sub>O<sub>3</sub> layer (identified in the following as Fe-Ba-DB); (iii) reverse double-bed configurations with BaO/Al<sub>2</sub>O<sub>3</sub> first, followed by a layer of either Fe-ZSM-5 or H-ZSM-5 (identified in the following as Ba-Fe-DB or Ba-Z-DB, respectively). In the double-bed configurations, the two phases were completely separated by a quartz wool plug, and each layer was diluted with cordierite up to 60 mg. For completeness, the three components (Fe-ZSM-5, BaO/Al<sub>2</sub>O<sub>3</sub> and H-ZSM-5) were also tested individually after dilution up to a total bed load of 120 mg.

Before running any test, each new sample was conditioned once for 5 h at 600 °C in a continuous flow of 10% v/v H<sub>2</sub>O and 10% v/v O<sub>2</sub> in He. Moreover, prior to every experiment the powders were pre-treated feeding 8% v/v O<sub>2</sub> + He at 550 °C continuously for 1 h and then also during the cool-down transient to the test temperature (120 °C). For brevity, illustration of the pre-treatment process is omitted in the results shown here: the data acquisition started (*t* = 0) when the desired test temperature was reached. The feed mixture to the reactor was composed from calibrated NO + He, NO<sub>2</sub> + He, NH<sub>3</sub> + He, O<sub>2</sub> + He mixtures in gas bottles using several mass flow controllers (Brooks Instruments). In particular, NO and O<sub>2</sub> were fed to the reactor via independent lines and mixed just before the reactor inlet, in order to prevent formation of NO<sub>2</sub> upstream of the catalyst bed. The purity of the mixtures was checked by a UV analyzer during preliminary calibrations. The gas species concentrations at the reactor outlet were analyzed by a quadrupole mass spectrometer (Balzers QMS 200) and a UV analyzer (ABB LIMAS 11 HW) arranged in a parallel configuration or, in an upgraded alternative set-up, using a new quadrupole mass spectrometer (Hiden Analytical QGA), which granted significant reduction of the signal noise. Cross-check experiments gave however essentially identical results in the two rigs.

The experimental protocol herein adopted is similar to the one described and validated in our previous works [12–14]. In general, three different types of transient gas-phase experiments were performed: (i) isothermal adsorption of a mixture of NO + O<sub>2</sub>, or NO<sub>2</sub> + O<sub>2</sub> or NO + NO<sub>2</sub> + O<sub>2</sub>, followed by Temperature Programmed Desorption (TPD) in He; (ii) isothermal adsorption of the same gas mixtures followed by Temperature Programmed Surface Reaction (TPSR) with NH<sub>3</sub>; (iii) isothermal adsorption of NH<sub>3</sub> followed by Temperature Programmed Surface Reaction (TPSR) with NO + NO<sub>2</sub>. Unless otherwise indicated, all the tests were run with an overall volumetric flow rate of 120 cm<sup>3</sup>/min (STP) at an adsorption temperature of 120 °C under dry conditions. Our previous works, in fact, pointed out a strong negative impact of H<sub>2</sub>O on the amount of NO<sub>x</sub> trapped on BaO due to its inhibitory action both on the NO oxidation activity of Fe-ZSM-5 [4], as also well known in the literature, and on the nitrites storage on BaO, documented e.g. by a dedicated experiment in [13]. Additional details regarding the experimental set-up and procedures, as well as the preparation and the characterization of the tested samples, can be found in [12–14].

## 3. Results and discussion

### 3.1. NO<sub>2</sub> + O<sub>2</sub> adsorption/TPD tests

In the isothermal adsorption phases, not shown here for brevity, 500 ppm of NO<sub>2</sub>, 8% O<sub>2</sub> and balance He were fed to the reactor until saturation at 120 °C. Fig. 1A shows the thermal decomposition (TPD) profiles of the NO<sub>x</sub> species stored on the investigated composite systems, namely Fe-Ba-MM, Fe-Ba-DB, and Ba-Fe-DB. For comparison, the results obtained in previous work [13] on the individually tested component phases are also displayed in Fig. 1B.

For all the three combined systems, Fig. 1A shows that the adsorbed NO<sub>x</sub> species decompose mainly to NO<sub>2</sub>, as expected in the case of nitrates storage [13,14]. The formation of stable nitrates

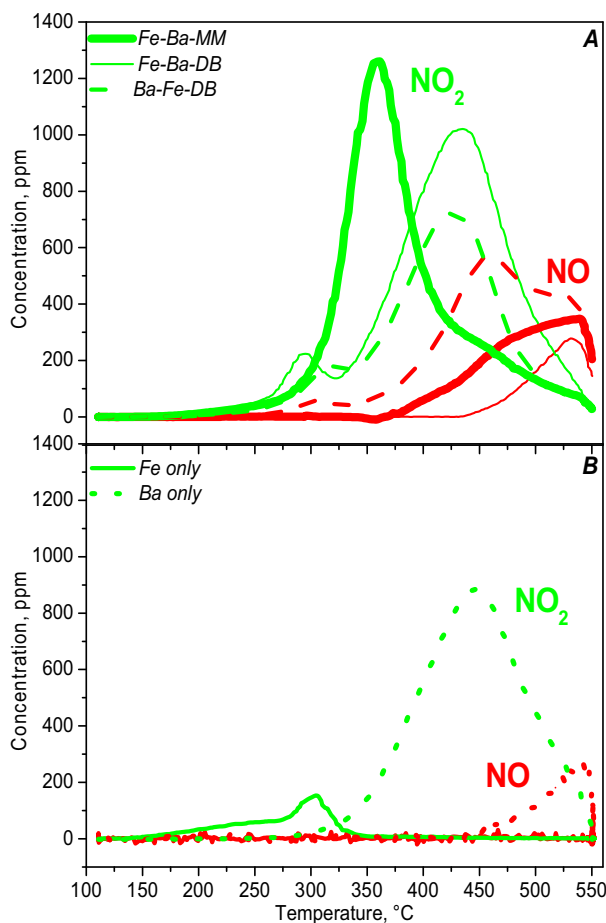


**Fig. 1.** TPD runs in He ( $T = 120\text{--}550\text{ }^{\circ}\text{C}$ ; heating rate =  $15\text{ }^{\circ}\text{C}/\text{min}$ ) following  $\text{NO}_2 + \text{O}_2$  adsorption at  $120\text{ }^{\circ}\text{C}$  ( $\text{NO}_2 = 500\text{ ppm}$ ;  $\text{O}_2 = 8\%$ ) on: (A) Fe-ZSM-5 +  $\text{BaO}/\text{Al}_2\text{O}_3$  in different configurations (thick lines: Fe-Ba-MM; thin lines: Fe-Ba-DB; dashed lines: Ba-Fe-DB); (B) individually tested Fe-ZSM-5 (solid lines) and  $\text{BaO}/\text{Al}_2\text{O}_3$  (dotted lines), reported for reference [13,14].

upon exposure of the same Fe-ZSM-5 catalyst to  $\text{NO}_2$  was in fact demonstrated by *in situ* FTIR in a previous dedicated study [16]. At temperatures above  $400\text{ }^{\circ}\text{C}$ , NO evolution is also detected, in line with the occurrence of  $\text{NO}_2$  decomposition to  $\text{NO} + \text{O}_2$  [13,14,17]. As already reported for mechanical mixture configurations [13,14], the  $\text{NO}_2$  TPD trace associated with Fe-Ba-MM (Fig. 1A, thick lines) exhibits a big peak (1260 ppm) centered at about  $360\text{ }^{\circ}\text{C}$ . Interestingly, this peak temperature is approximately  $90\text{ }^{\circ}\text{C}$  lower than the one registered in the same  $\text{NO}_2$  adsorption experiment on  $\text{BaO}/\text{Al}_2\text{O}_3$  alone ( $450\text{ }^{\circ}\text{C}$ ), see Fig. 1B. Thus, the thermal stability of barium nitrates is less in the mechanical mixture configuration, likely due to the presence of the iron sites. In fact, as also evident in Fig. 1B, Fe nitrates start to decompose at lower temperatures (around  $200\text{ }^{\circ}\text{C}$ ), freeing active sites that may act as additional decomposition centers for nitrates stored on  $\text{BaO}/\text{Al}_2\text{O}_3$ . This is clear evidence for an interaction between the two mixture components, and strongly suggests that Ba- and Fe-nitrates are both in equilibrium with a mediating gas-phase species, possibly  $\text{HNO}_3$  or  $\text{NO}_2$ .

Upon separating the mixture components in two segregated beds, with Fe-ZSM-5 upstream of  $\text{BaO}/\text{Al}_2\text{O}_3$  (Fe-Ba-DB), the  $\text{NO}_2$  TPD trace was changed to a bimodal profile with a first peak of 220 ppm at  $300\text{ }^{\circ}\text{C}$  and a second one of 1020 ppm at  $435\text{ }^{\circ}\text{C}$  (Fig. 1A, thin lines). In this double bed configuration, therefore, the two components behave independently, with two separate nitrates decomposition peaks corresponding nicely to those observed on

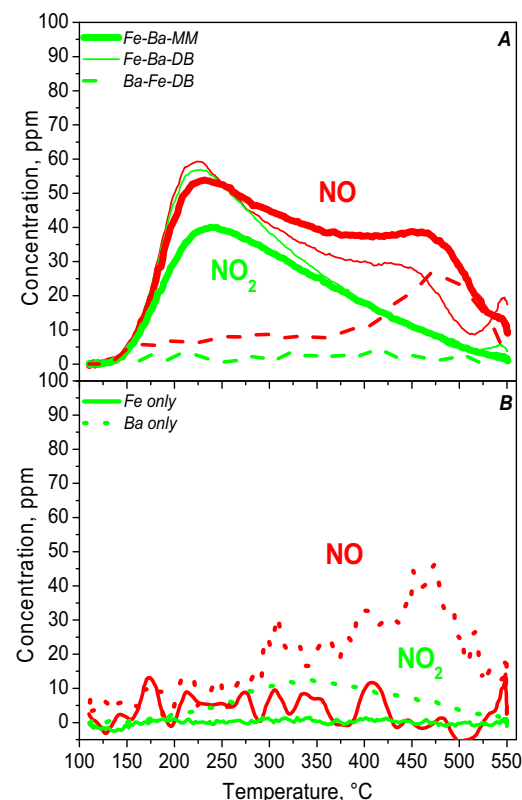


**Fig. 2.** TPD runs in He ( $T = 120\text{--}550\text{ }^{\circ}\text{C}$ ; heating rate =  $15\text{ }^{\circ}\text{C}/\text{min}$ ) following  $\text{NO} + \text{O}_2$  adsorption at  $120\text{ }^{\circ}\text{C}$  ( $\text{NO} = 500\text{ ppm}$ ;  $\text{O}_2 = 8\%$ ) on: (A) Fe-ZSM-5 +  $\text{BaO}/\text{Al}_2\text{O}_3$  in different configurations (thick lines: Fe-Ba-MM; thin lines: Fe-Ba-DB; dashed lines: Ba-Fe-DB); (B) individually tested Fe-ZSM-5 (solid lines) and  $\text{BaO}/\text{Al}_2\text{O}_3$  (dotted lines), reported for reference [12,13].

the individually tested systems, shown in Fig. 1B. In this case, no interaction is evident: on the contrary, the  $\text{NO}_2$  TPD profile is just the superposition of those obtained on the two single components, which is indeed consistent with the arrangement of the two layers in the Fe-Ba-DB system. In fact, the Fe-ZSM-5 bed is positioned upstream, so, unlike in the mechanical mixture, the redox metal sites cannot act as decomposition centers for the stable Ba nitrates, which are stored in the downstream layer. Indeed, the synergistic effect is absent also when reversing the order of the layers (Ba-Fe-DB), as clearly seen in Fig. 1A (dashed lines). Again, phase separation prevents the shift of the local nitrates decomposition equilibrium, differently from the case of the mechanical mixture (Fe-Ba-MM). The different  $\text{NO}_2$  release concentrations noted e.g. between  $\text{BaO}/\text{Al}_2\text{O}_3$  and Ba-Fe-DB are likely explained by the differences in the overall  $\text{NO}_x$  storage capacity of  $\text{BaO}/\text{Al}_2\text{O}_3$  samples from replicated preparations.

In summary, the  $\text{NO}_2$  adsorption/TPD tests point out a significant interaction between the two component phases of our composite systems during nitrates decomposition, but only in the case of Fe-Ba-MM. In fact, the nitrates stored onto BaO are more easily decomposed only when BaO is mixed with Fe-ZSM-5. Such an interaction apparently requires proximity of the Fe decomposition sites to the BaO storage sites.

### 3.2. $\text{NO} + \text{O}_2$ adsorption/TPD tests

In the isothermal adsorption phases of these experiments, not shown here for brevity, 500 ppm of NO with 8%  $\text{O}_2$  and balance He were fed to the reactor until saturation at  $120\text{ }^{\circ}\text{C}$ . Fig. 2A shows the TPD profiles of the  $\text{NO}_x$  species stored on the investigated composite systems, i.e. Fe-Ba-MM, Fe-Ba-DB, and Ba-Fe-DB, after exposure

to  $\text{NO} + \text{O}_2$ . For comparison, the corresponding results obtained in previous work [12–14] on the individually tested components are also displayed in Fig. 2B. Contrary to the case of  $\text{NO}_2$  adsorption, the stored NOx species exhibit here the typical thermal decomposition behavior of nitrites, i.e. equimolar release of NO and  $\text{NO}_2$  in the low temperature region [12–14], with the exception of the Ba-Fe-DB configuration, explained later.

As also discussed extensively in [12–15], a clear synergistic interaction between Fe-ZSM-5 and  $\text{BaO}/\text{Al}_2\text{O}_3$  is again evident when comparing the mechanical mixture (Fe-Ba-MM) in Fig. 2A (thick lines) to the individual components, reported for reference in Fig. 2B. The NO and  $\text{NO}_2$  TPD traces are overlapped until 180 °C, with a main peak at 225 °C. These results are explained considering that NO is oxidatively activated on Fe sites and the generated intermediates are trapped on the  $\text{BaO}/\text{Al}_2\text{O}_3$  phase in the form of barium nitrites. Indeed, Fig. 2B clearly confirms that the NOx storage on the two individual components is quite small: in fact, Fe-ZSM-5 is not able to stabilize nitrites which easily decompose, while  $\text{BaO}/\text{Al}_2\text{O}_3$  has a very limited oxidation activity and is thus unable to activate NO.

When  $\text{NO} + \text{O}_2$  adsorption was replicated on the Fe-ZSM-5 +  $\text{BaO}/\text{Al}_2\text{O}_3$  double bed configuration (Fe-Ba-DB, see Fig. 2A, thin lines), almost identical decomposition profiles were obtained as over the mechanical mixture (Fe-Ba-MM): NO and  $\text{NO}_2$  were released in perfect equimolar proportions up to 300 °C, with a peak of about 60 ppm each at 225 °C. Thus, remarkably, the synergy between the Fe-ZSM-5 catalyst and  $\text{BaO}/\text{Al}_2\text{O}_3$  during  $\text{NO} + \text{O}_2$  adsorption is completely unaffected by the segregation of the two phases. This implies that the interaction proceeds via the gas phase and is mediated by a stable molecule, which is obviously a nitrite precursor and therefore different from the  $\text{NO}_2$  adsorption case. These results are apparently at variance with those obtained by Salazar et al. [18] on hybrid catalysts containing an oxidation component (e.g.  $\text{Mn}_2\text{O}_3$ , hopcalite and  $\text{Ce-ZrO}_x$ ) and an SCR component (Fe-ZSM-5,  $\text{V}_2\text{O}_5$ - $\text{WO}_3$ / $\text{TiO}_2$ ) arranged in either physical mixtures or segregated configurations. In their work, the authors observed a strong increase of the Standard SCR performances on the combined system with close contact between the two phases, possibly due to the beneficial effect of the oxidation component in the oxidative activation of NO. However, the synergy was strongly reduced in a loose contact physical mixture and completely absent in more segregated configurations, suggesting that the interaction, in this case, was mediated by a labile intermediate [18].

Finally, upon reversing the order of the layers (Ba-Fe-DB) in Fig. 2A (dashed lines), no significant storage of nitrites was noted, as expected also from previous results [13]. In this case, the TPD curves look very similar to those shown in Fig. 2B for the individual systems. In fact, here Fe-ZSM-5 is placed downstream of the storage material, which prevents trapping of any nitrites precursors formed over the oxidative component.

Thus, oxidative activation of NO at 120 °C over Fe-ZSM-5 generates a stable gas-phase nitrite precursor, which can travel a significant distance across the reactor to reach the segregated BaO component downstream, and is eventually trapped as a stable Ba nitrite. At this point, of course, the question is about the nature of such a mediating gaseous species, which could possibly be  $\text{NO}_2$ ,  $\text{N}_2\text{O}_3$  or HONO [7,8,12–14]. The answer is quite relevant for the elucidation of the Standard SCR mechanism.

### 3.3. $\text{NO} + \text{NO}_2 + \text{O}_2$ adsorption/TPD tests

The following experiment was performed to gain insight in the nature of the gas-phase species mediating the synergy of combined Fe-ZSM-5 +  $\text{BaO}/\text{Al}_2\text{O}_3$  systems in  $\text{NO} + \text{O}_2$  adsorption. The Fe-zeolite catalyst, whose role is to oxidatively activate NO, was removed from the tested system and its functionality was replaced

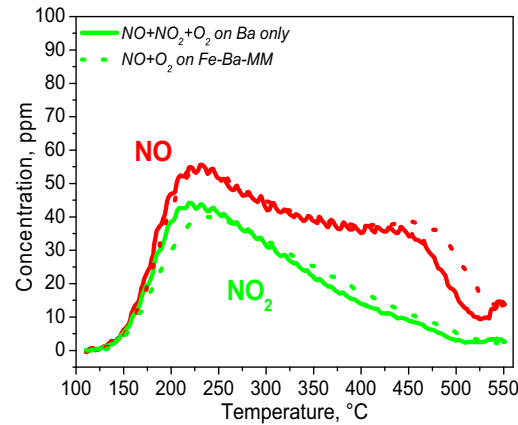


**Fig. 3.** TPD runs in He ( $T=120\text{--}550^\circ\text{C}$ ; heating rate = 15 °C/min) following  $\text{NO} + \text{NO}_2 + \text{O}_2$  adsorption at 120 °C (NO = 500 ppm;  $\text{NO}_2$  = 50 ppm;  $\text{O}_2$  = 8%, exposure time = 45 min) on  $\text{BaO}/\text{Al}_2\text{O}_3$  only (solid lines) and  $\text{NO} + \text{O}_2$  adsorption at 120 °C (NO = 500 ppm;  $\text{O}_2$  = 8%) on Fe-ZSM-5 +  $\text{BaO}/\text{Al}_2\text{O}_3$  physical mixture (Fe-Ba-MM, dotted lines), respectively.

by adding 50 ppm of  $\text{NO}_2$  to the 500 ppm  $\text{NO} + 8\%$   $\text{O}_2$  mixture fed to  $\text{BaO}/\text{Al}_2\text{O}_3$  only. This was the minimum concentration of  $\text{NO}_2$  that could be fed to the reactor due to experimental constraints: it is, however, in the same order of magnitude of the steady-state outlet  $\text{NO}_2$  concentration generated by the NO oxidation activity of the Fe-BaO physical mixture [12,13]. The TPD curves following  $\text{NO} + \text{NO}_2 + \text{O}_2$  adsorption on  $\text{BaO}/\text{Al}_2\text{O}_3$  are plotted in Fig. 3 as solid lines. NO and  $\text{NO}_2$  were desorbed in equimolar amounts up to 180 °C, with synchronous peaks at 225 °C, again in line with nitrites thermal decomposition. This confirms that exposure to a mixture of  $\text{NO}_2$  in excess NO can form nitrites on  $\text{BaO}/\text{Al}_2\text{O}_3$ , as already pointed out by Iglesia et al. [19]. It is also worth noticing here that the duration of  $\text{NO} + \text{NO}_2$  adsorption on  $\text{BaO}/\text{Al}_2\text{O}_3$  was controlled and limited to 45 min to prevent the consecutive oxidation of the trapped nitrites to nitrates by  $\text{NO}_2$  [19], see Section 3.5 below. Notably, we can also rule out the initial formation of nitrates on  $\text{BaO}/\text{Al}_2\text{O}_3$  and their subsequent reduction by NO to nitrites based on a dedicated test, already presented in [13]. In this test, a single bed of  $\text{BaO}/\text{Al}_2\text{O}_3$  was first saturated with nitrates at 120 °C, and subsequently exposed to 500 ppm of NO without observing any appreciable reaction.

As a most interesting and surprising result, however, Fig. 3 further shows that the TPD curves recorded after  $\text{NO} + \text{NO}_2 + \text{O}_2$  isothermal adsorption on  $\text{BaO}/\text{Al}_2\text{O}_3$  (solid lines) almost perfectly match the TPD curves obtained following  $\text{NO} + \text{O}_2$  adsorption on the Fe-Ba-MM physical mixture, also displayed as dotted lines for comparison. Thus, adsorption of  $\text{NO}_2$  in excess NO on the BaO phase alone results in a storage of nitrites that is both qualitatively and quantitatively similar to what observed in  $\text{NO} + \text{O}_2$  adsorption runs on both mechanical mixture (Fe-Ba-MM) and double-bed (Fe-Ba-DB) systems. The simplest possible explanation of this new compelling result is that the role of Fe sites in Fe-ZSM-5 is to oxidize NO to  $\text{NO}_2$ . According to this interpretation,  $\text{NO}_2$  would be therefore the stable mediating gaseous species involved in the interaction between Fe-ZSM-5 and  $\text{BaO}/\text{Al}_2\text{O}_3$  pointed out in the previous paragraphs.

Another experiment apparently corroborating this interpretation is presented in Fig. 4. It involves an isothermal step feed of 2%  $\text{O}_2$  during continuous feed of NO at 120 °C on Fe-ZSM-5 only (dashed lines) and on the Fe-ZSM-5 +  $\text{BaO}/\text{Al}_2\text{O}_3$  double bed system (Fe-Ba-DB, solid lines). Fig. 4 shows that as soon as oxygen was fed to Fe-ZSM-5, approximately 50 ppm of NO were converted and

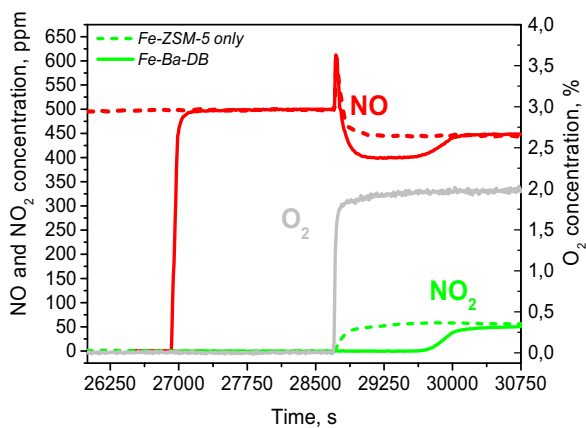


**Fig. 4.**  $O_2$  step feed during NO isothermal adsorption ( $T = 120^\circ\text{C}$ ;  $\text{NO} = 500 \text{ ppm}$ ;  $O_2 = 2\%$ ) on Fe-ZSM-5 + BaO/Al<sub>2</sub>O<sub>3</sub> double bed (solid lines) and on Fe-ZSM-5 only (dashed lines).

50 ppm of  $\text{NO}_2$  were produced, in line with the occurrence of NO oxidation, (R1) [12,13]:



When the same experiment was run on Fe-Ba-DB, different, peculiar dynamics were observed: the NO outlet concentration first dropped to 400 ppm and then, after a transient, recovered the same steady state value noticed in the case of Fe-ZSM-5 only ( $\approx 450 \text{ ppm}$ ). This is quantitatively in line with one molecule of NO being oxidized to  $\text{NO}_2$  on the Fe-zeolite, (R1), which is then trapped, together with one additional NO molecule, as barium nitrite in the BaO-Al<sub>2</sub>O<sub>3</sub> bed downstream according to (R2), until saturation equilibrium is reached:



Integral analysis confirmed storage of similar amounts of NOx after the  $\text{NO} + \text{O}_2$  adsorption on Fe-Ba-DB (Fig. 4), the  $\text{NO} + \text{O}_2$  adsorption on Fe-Ba-MM (Fig. 2), and the  $\text{NO} + \text{NO}_2 + \text{O}_2$  adsorption on BaO/Al<sub>2</sub>O<sub>3</sub> (Fig. 3).

#### 3.4. Discussion on the nature of the intermediate species in $\text{NO} + \text{O}_2$ adsorption

Even though the new results presented in the previous paragraphs apparently suggest that  $\text{NO}_2$  acts as the mediating species between Fe-ZSM-5 and BaO, we believe that the identification of the intermediate formed by the oxidative activation of NO over Fe-zeolites is not so straightforward and deserves some more detailed discussion. Indeed, the simple scheme with NO oxidation to  $\text{NO}_2$  as the rate determining step of Standard SCR has been questioned in the past by some of us on the basis of multiple kinetic pieces of evidence [4].

Our present data tell clearly that the intermediate generated by NO oxidation on Fe-centers has to be a nitrite precursor, since its interaction with BaO results in the formation of nitrites as primary adsorbed species [13,14]. In the  $\text{NO}_2$  molecule, however, N has a formal oxidation state of 4+, while in nitrites N has a formal oxidation state of 3+, so pure  $\text{NO}_2$  cannot be a direct precursor of nitrites. In the adsorption of  $\text{NO}_2$  alone, in fact,  $\text{NO}_2$  disproportionates to form both nitrites and nitrates, as discussed e.g. in [16]. However, the results of our  $\text{NO}_2 + \text{NO}$  adsorption runs on BaO/Al<sub>2</sub>O<sub>3</sub> show that  $\text{NO}_2$  in the presence of excess NO behaves indeed as a nitrite precursor. A possible explanation is that  $\text{NO}_2$  in excess NO is in equilibrium with  $\text{N}_2\text{O}_3$ , whose N atoms share a formal oxidation state of 3+, like in nitrites. Furthermore, in presence of  $\text{H}_2\text{O}$ , which

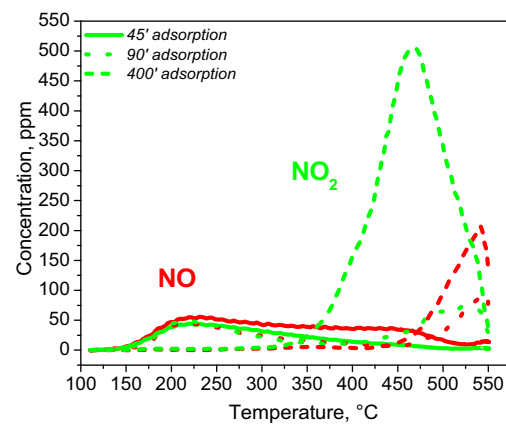


**Fig. 5.** TPD runs in He ( $T = 120\text{--}550^\circ\text{C}$ ; heating rate =  $15^\circ\text{C}/\text{min}$ ) following  $\text{NO} + \text{NO}_2 + \text{O}_2$  adsorption ( $\text{NO} = 500 \text{ ppm}$ ;  $\text{NO}_2 = 50 \text{ ppm}$ ;  $\text{O}_2 = 8\%$ ) at  $120^\circ\text{C}$  on BaO/Al<sub>2</sub>O<sub>3</sub> with different exposure times (thick lines: 45 min; dotted lines: 90 min; dashed lines: 400 min).

cannot be excluded in zeolites even in dry experiments like ours,  $\text{NO}_2 + \text{NO}$  may be in equilibrium both with  $\text{N}_2\text{O}_3$  and with HONO, also a nitrite precursor.

If such equilibria apply, then it seems hardly possible to establish if: (i) NO is first activated on Fe to form ferric nitrites in equilibrium with gaseous  $\text{N}_2\text{O}_3/\text{HONO}$ , and subsequently  $\text{N}_2\text{O}_3/\text{HONO}$  is stored on BaO as nitrites, or (ii) NO is first oxidized to  $\text{NO}_2$  on Fe sites, and then  $\text{NO} + \text{NO}_2$  are stored on BaO as nitrites. In the future, a kinetic analysis could be attempted to discriminate the two pathways, considering that they might also proceed in parallel.

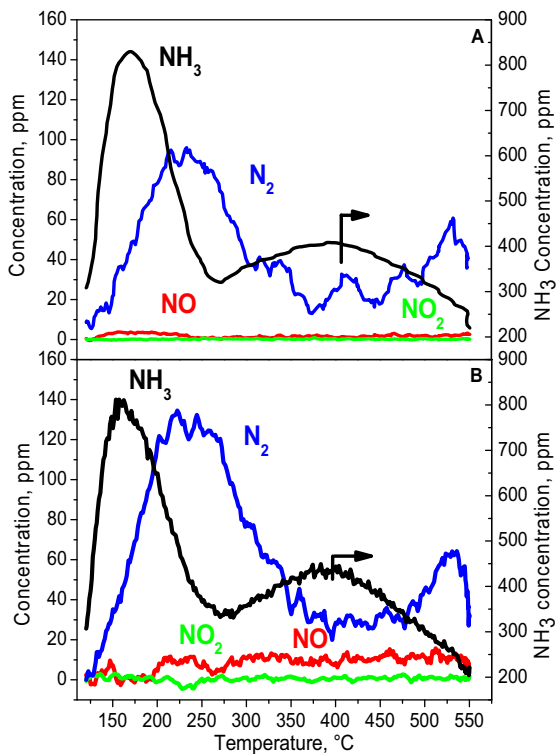
#### 3.5. Evolution of Ba-nitrites

Fig. 5 compares three TPD profiles following  $\text{NO} + \text{NO}_2 + \text{O}_2$  adsorption on BaO/Al<sub>2</sub>O<sub>3</sub> with different exposure times. It is evident that, on progressively increasing the adsorption time (from 45 to 400 min), the low-temperature equimolar NO and  $\text{NO}_2$  peak, associated with nitrites decomposition, decreased, while two new  $\text{NO}_2$  and NO peaks appeared in the high-T region (centered at  $525^\circ\text{C}$  and  $550^\circ\text{C}$ , respectively), associated with the thermal decomposition of stable nitrates to  $\text{NO}_2$ , which further decomposes to NO +  $\text{O}_2$ . Accordingly, Fig. 5 highlights the shift towards nitrates with growing  $\text{NO} + \text{NO}_2$  adsorption time on BaO/Al<sub>2</sub>O<sub>3</sub> likely due to the consecutive oxidation of the initially formed nitrites by  $\text{NO}_2$ , in line with literature indications from Iglesia et al. [19].

#### 3.6. NH<sub>3</sub> reactivity tests

At this point, we look at the subsequent step in the low-temperature Standard SCR chemistry: after NO oxidative activation, the NOx intermediate proceeds to react with NH<sub>3</sub> to form dinitrogen.

We probed the reactivity with NH<sub>3</sub> of nitrites accumulated onto BaO/Al<sub>2</sub>O<sub>3</sub> in  $\text{NO} + \text{NO}_2 + \text{O}_2$  adsorption tests in NH<sub>3</sub>-TPSR experiments on two distinct inverted double bed arrangements, namely Ba-Fe-DB and Ba-Z-DB. In the isothermal adsorption phase of these runs, 500 ppm of NO, 50 ppm of  $\text{NO}_2$  and 8%  $\text{O}_2$  were fed at  $120^\circ\text{C}$  for a controlled time (45 min) to prevent consecutive oxidation of nitrites to nitrates by  $\text{NO}_2$  [19], see also the discussion of Fig. 5. In the second phase, 300 ppm of NH<sub>3</sub> were fed to the reactor at  $120^\circ\text{C}$  until steady state was reached, then the temperature was raised up to  $550^\circ\text{C}$  at  $15^\circ\text{C}/\text{min}$ . Fig. 6A shows the subsequent TPSR for the BaO/Al<sub>2</sub>O<sub>3</sub> + Fe-ZSM-5 double bed configuration (Ba-Fe-DB). As soon as the temperature was increased, N<sub>2</sub> evolution was detected with a peak of approximately 90 ppm at  $235^\circ\text{C}$ . At



**Fig. 6.** TPSR runs in  $\text{NH}_3$  ( $\text{NH}_3 = 300 \text{ ppm}$ ;  $T = 120\text{--}550^\circ\text{C}$ ; heating rate =  $15^\circ\text{C}/\text{min}$ ) following  $\text{NO} + \text{NO}_2 + \text{O}_2$  adsorption at  $120^\circ\text{C}$  ( $\text{NO} = 500 \text{ ppm}$ ;  $\text{NO}_2 = 50 \text{ ppm}$ ;  $\text{O}_2 = 8\%$ ) on: (A) Ba-Fe-DB; (B) Ba-Z-DB.

the same time,  $\text{NH}_3$  consumption was also observed. The integral amount of produced  $\text{N}_2$  ( $7.28 \mu\text{mol}$ ) is consistent with the overall stored  $\text{NO} + \text{NO}_2$ , evaluated in a dedicated TPD run ( $7.84 \mu\text{mol}$ ), with a balance error below 8%, in line with the well-known Fast SCR stoichiometry, (R3):

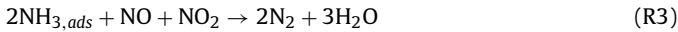
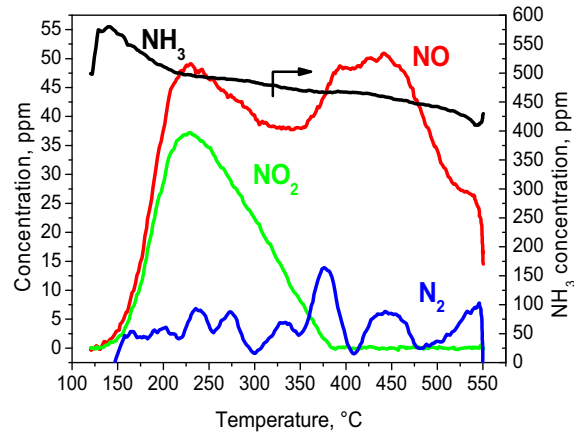


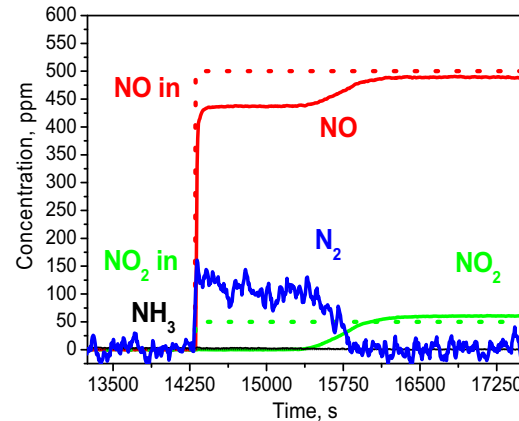
Fig. 6B shows further that a very similar result was found when replacing Fe-ZSM-5 with H-ZSM-5 in the double bed arrangement (Ba-Z-DB). Again, a low temperature  $\text{N}_2$  peak of 125 ppm at  $235^\circ\text{C}$ , even more abundant than in the previous case, was detected. Also in this case, a limited additional  $\text{N}_2$  production peak was noticed at high temperature: this may be explained by the reaction of  $\text{NH}_3$  with some nitrates generated by the  $\text{NO}_2$  conversion of nitrites, as shown e.g. in Fig. 5. Notice that, in both cases, no  $\text{N}_2$  was detected when  $\text{NH}_3$  was fed to the reactor before starting the ramp, being the temperature ( $120^\circ\text{C}$ ) too low to initiate nitrites decomposition from the  $\text{BaO}/\text{Al}_2\text{O}_3$  phase.

The low temperature reactivity with  $\text{NH}_3$  noted in the previous tests is typical of nitrites, as well known and already discussed in previous chemical trapping work [12–15] on physical mixtures: we show here that it is still present in a configuration with segregated beds. Notice that only limited  $\text{NH}_3$  storage and, most importantly, insignificant  $\text{NH}_3$  reactivity were observed on the  $\text{BaO}/\text{Al}_2\text{O}_3$  phase when tested alone in the dedicated test presented in Fig. 7 below.

The  $\text{NH}_3$ -TPSR data in Fig. 6 are strong evidence that the equimolar mixture of  $\text{NO}$  and  $\text{NO}_2$  from decomposition of barium nitrites stored on  $\text{BaO}/\text{Al}_2\text{O}_3$  readily reacts with the ammonia adsorbed on the zeolite acid sites downstream. In fact, the behaviors of the two tested samples, namely Ba-Fe-DB and Ba-Z-DB, are essentially identical, even though the Fe contents of the two zeolites differ by two orders of magnitude. Moreover, the reactivity is quite significant, leading to a complete conversion of the stored species, despite the very low temperature. Clearly, such a very effective reactivity is to



**Fig. 7.** TPSR run in  $\text{NH}_3$  ( $\text{NH}_3 = 500 \text{ ppm}$ ;  $T = 120\text{--}550^\circ\text{C}$ ; heating rate =  $15^\circ\text{C}/\text{min}$ ) following  $\text{NO} + \text{NO}_2 + \text{O}_2$  adsorption ( $\text{NO} = 500 \text{ ppm}$ ;  $\text{NO}_2 = 50 \text{ ppm}$ ;  $\text{O}_2 = 8\%$ ) at  $120^\circ\text{C}$  on  $\text{BaO}/\text{Al}_2\text{O}_3$ .

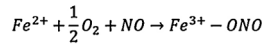
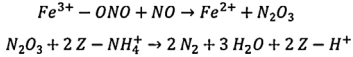
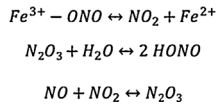


**Fig. 8.** Step feed of  $\text{NO} + \text{NO}_2$  ( $\text{NO} = 500 \text{ ppm}$ ;  $\text{NO}_2 = 50 \text{ ppm}$ ;  $T = 120^\circ\text{C}$ ;) following  $\text{NH}_3$  adsorption at  $120^\circ\text{C}$  ( $\text{NH}_3 = 500 \text{ ppm}$ ) on H-ZSM5.

be attributed to the  $\text{NH}_3$  adsorbed on the zeolite acid sites, whereas the role of the  $\text{NH}_3$  interaction with the Fe redox sites seems to be very limited at these conditions.

To further confirm these results, one additional, dual test was run on H-ZSM-5 only. The parent zeolite was first saturated with  $\text{NH}_3$  at  $120^\circ\text{C}$  (not shown for brevity) and then, after  $\text{NH}_3$  shutoff, a mixture of 500 ppm of  $\text{NO}$  and 50 ppm of  $\text{NO}_2$  was fed to the reactor, still at the same temperature. Fig. 8 shows the following isothermal transient: it is evident that, as soon as the  $\text{NOx}$  mixture was contacted with adsorbed  $\text{NH}_3$ , already at  $120^\circ\text{C}$   $\text{NO}_2$ , i.e. the limiting reactant, was fully converted to  $\text{N}_2$ . The corresponding  $\text{NO}$  conversion and  $\text{N}_2$  release were in line with the stoichiometry of Fast SCR, Reaction (R3). Of course, after some time the preadsorbed  $\text{NH}_3$  was depleted, and both  $\text{NO}$  and  $\text{NO}_2$  eventually approached their steady-state levels. It is thus possible to conclude that  $\text{NO} + \text{NO}_2$  in equilibrium with nitrites react with adsorbed  $\text{NH}_3$  already at very low temperatures and with extremely fast rates.

Another important implication is that, at our investigated conditions, the formation of  $\text{N}_2$  from  $\text{NH}_3 + \text{NO} + \text{NO}_2$  may not necessarily require any oxidative activation of ammonia, given the extremely limited amount of Fe centers available on the H-ZSM-5 sample. This is consistent with data reported by Stakheev et al. [20] and by Ellmers et al. [21], showing the Fast SCR reaction to proceed on catalytic systems virtually free of redox sites. We are aware of the role of Fe impurities in determining the SCR activity of technical parent zeolites [21], such as the one used in this study. It is

Oxidation half cycle:Reduction half cycle:In addition:**Fig. 9.** Proposed redox chemistry for Standard SCR over Fe-zeolites.

worth emphasizing however that, in spite of a 40-times smaller load of iron in H-ZSM-5 than in the Fe-ZSM-5 catalyst, we obtained essentially the same high conversion activity observed on the Fe-promoted system already at low temperatures, as documented in Fig. 6. This seems therefore hardly compatible with a mechanism requiring the oxidative activation of NH<sub>3</sub> on Fe centers.

The very simple scheme in Fig. 9 provides a redox cycle, which is consistent with all the observations reported in this work.

Here, the reduced Fe sites are oxidized by oxygen and NO to form ferric nitrites, whose reductive decomposition leads to the release of NO<sub>2</sub>, in equilibrium with N<sub>2</sub>O<sub>3</sub> together with NO. In the presence of BaO, N<sub>2</sub>O<sub>3</sub> will form Barium nitrites. In the presence of ammonia adsorbed on the zeolite acid sites, instead, N<sub>2</sub>O<sub>3</sub> will form unstable ammonium nitrite, rapidly resulting in the evolution of N<sub>2</sub> and H<sub>2</sub>O. Notably, this latter step does not involve any redox functionality, in agreement with our results in this section. It is also worth pointing out that NO<sub>2</sub> appears explicitly neither in the oxidation nor in the reduction half cycle in Fig. 9. NO oxidative activation leading to the reduction of Fe<sup>3+</sup> in Fe-ZSM-5 has been observed by Boubnov et al. [22] by operando HERFD-XANES.

## 4. Conclusions

On investigating the effect of phase separation in Fe-ZSM-5 + BaO/Al<sub>2</sub>O<sub>3</sub> combined systems exposed to NO/NO<sub>2</sub> + O<sub>2</sub> mixtures at 120 °C, we have collected a number of novel results which shed light on the NH<sub>3</sub>-SCR catalytic chemistry over metal-promoted zeolites.

Our new data confirm the strong interaction between Fe-ZSM-5 and BaO/Al<sub>2</sub>O<sub>3</sub>, already documented in [12–14], but further prove that this proceeds via the gas phase. For NO + O<sub>2</sub> adsorption, in particular, the interaction is mediated by stable molecules, which act as nitrite precursors, resulting in nitrites storage on BaO, and are able to travel across the reactor even in the case of a fully segregated double bed configuration.

Concerning the nature of such mediating gaseous species, we have observed striking similarities between NO + O<sub>2</sub> adsorption on the Fe-ZSM-5 + BaO/Al<sub>2</sub>O<sub>3</sub> mechanical mixture and NO<sub>2</sub> adsorption in excess NO on the sole BaO/Al<sub>2</sub>O<sub>3</sub> phase. Therefore, it is tempting to conclude that the relevant mediating species is just NO<sub>2</sub>. Indeed, while NO<sub>2</sub> alone has a formal N oxidation state of +4, we have shown that NO<sub>2</sub> in excess NO behaves instead as a nitrite precursor, i.e. with an N oxidation state of +3. We cannot rule out therefore that the gaseous intermediate generated by NO oxidation over Fe-ZSM-5 is actually another molecule with a formal N oxidation state of +3, like N<sub>2</sub>O<sub>3</sub> or HONO. It is also possible that all such species, namely NO + NO<sub>2</sub>, N<sub>2</sub>O<sub>3</sub>, HONO, are in equilibrium with each other, being eventually indistinguishable from a mechanistic and kinetic point of view. Regardless of the exact nature of the gaseous intermediate, our data point out very clearly that a crucial redox step in the Stan-

dard SCR mechanism at low temperatures involves the oxidation of the N atom in NO to a state of +3.

In addition, we have shown that nitrites generated by the oxidative activation of NO on Fe-ZSM-5 and stored on BaO react readily with NH<sub>3</sub> adsorbed on the zeolite acid sites via their decomposition to NO + NO<sub>2</sub>. Most important, such a reactivity proceeds regardless of the concentration of redox metal sites on the zeolite: in fact, we have observed a quite comparable NH<sub>3</sub> reactivity with NO + NO<sub>2</sub> on Fe-ZSM-5 and on H-ZSM-5, in spite of the drastically reduced Fe content of the latter sample.

Altogether, the experiments herein presented mimic the two sequential steps of one possible low-temperature mechanistic pathway for the Standard SCR reaction over Fe-zeolites. In this bi-functional mechanism, the oxidative activation of NO on the Fe-sites provides the NO<sub>2</sub>/N<sub>2</sub>O<sub>3</sub>/HONO gaseous reactive intermediates, which are then rapidly reduced to dinitrogen by the ammonia adsorbed on the catalyst acid sites. On the other hand, the oxidative activation of NH<sub>3</sub> was notably not necessary in our experiments in order to reduce NO to dinitrogen at 120 °C. While we cannot rule out other surface pathways, this gas-phase mediated route was found quite active and compelling at our experimental conditions.

Altogether, the present data suggest strong analogies with the Standard SCR mechanism postulated by Stakheev et al. [20] for their bifunctional Combicat systems, wherein one oxidative component is deemed responsible for the oxidation of NO to NO<sub>2</sub>, while the other component, associated with acidic properties but not necessarily possessing redox properties, sustains the Fast SCR reactivity between NO, NO<sub>2</sub> and NH<sub>3</sub>. In our experiments, however, both functionalities have been demonstrated for the same Fe-zeolite SCR catalyst. The novel evidence herein collected also emphasizes the often-overlooked potential relevance of gas-phase intermediates in the Standard SCR reaction over metal-promoted zeolites.

In all the present experiments, water was not added to the feed stream to the reactor, even though it is of course an important component of real engine exhausts, because we learnt from previous work [13] that water would significantly hamper the NO<sub>x</sub> storage capability of BaO, and thus the efficiency of our chemical trapping techniques. A dedicated study of the H<sub>2</sub>O effect will be reported however in the near future.

## Acknowledgments

The authors acknowledge Mauro Fiorito and Alessandro Molina for the experimental work and for fervent discussions. ET is indebted to Wolfgang Grünert, Alexandr Stakheev and Alina Mytareva for stimulating discussions and critical suggestions.

## References

- [1] S. Brandenberger, O. Kröcher, A. Tissler, R. Althoff, *Catal. Rev.—Sci. Eng.* 50 (2008) 492–531.
- [2] I. Ellmers, R.P. Vélez, U. Bentrup, A. Brückner, W. Grünert, *J. Catal.* 311 (2014) 199–211.
- [3] A. Grossale, I. Nova, E. Tronconi, D. Chatterjee, M. Weibel, *J. Catal.* 256 (2008) 312–322.
- [4] M.P. Ruggeri, I. Nova, E. Tronconi, *Top. Catal.* 56 (2013) 109–113.
- [5] A. Savara, M.-J. Li, W.M.H. Sachtler, E. Weitz, *Appl. Catal. B: Environ.* 81 (2008) 251–257.
- [6] A. Savara, W.M.H. Sachtler, E. Weitz, *Appl. Catal. B: Environ.* 90 (2009) 120–125.
- [7] Y.H. Yeom, J. Henao, M.J. Li, W.M.H. Sachtler, E. Weitz, *J. Catal.* 231 (2005) 181–193.
- [8] J.H. Kwak, J.H. Lee, S.D. Burton, A.S. Lipton, C.H.F. Peden, J. Szanyi, *Angew. Chem.—Int. Ed.* 52 (2013) 9985–9989.
- [9] C. Paolucci, A.A. Verma, S.A. Bates, V.F. Kispersky, J.T. Miller, R. Gounder, W.N. Delgass, F.H. Ribeiro, W.F. Schneider, *Angew. Chem.* (2014) 11828–11833.
- [10] T.V.W. Janssens, H. Falsig, L.F. Lundsgaard, P.N.R. Vennestrøm, S.B. Rasmussen, P.G. Moses, F. Giordanino, E. Borfecchia, K.A. Lomachenko, C. Lamberti, S. Bordiga, A. Godiksen, S. Mossin, P. Beato, *ACS Catal.* 5 (2015) 2832–2845.
- [11] M. Schmidder, S. Heikens, A. De Toni, S. Geisler, M. Berndt, A. Brückner, W. Grünert, *J. Catal.* 259 (2008) 96–103.

- [12] M.P. Ruggeri, T. Selleri, M. Colombo, I. Nova, E. Tronconi, *J. Catal.* 311 (2014) 266–270.
- [13] M.P. Ruggeri, T. Selleri, M. Colombo, I. Nova, E. Tronconi, *J. Catal.* 328 (2015) 258–269.
- [14] T. Selleri, M.P. Ruggeri, I. Nova, E. Tronconi, *Top. Catal.* 59 (2016) 678–685.
- [15] M.P. Ruggeri, T. Selleri, I. Nova, E. Tronconi, J.A. Pihl, T.J. Toops, W.P. Partridge, *Top. Catal.* 59 (2016) 907–912.
- [16] M.P. Ruggeri, A. Grossale, I. Nova, E. Tronconi, H. Jirglova, Z. Sobalik, *Catal. Today* 184 (2012) 107–114.
- [17] M. Colombo, I. Nova, E. Tronconi, *Appl. Catal. B: Environ.* 111–112 (2012) 433–444.
- [18] M. Salazar, S. Hoffmann, O.P. Tkachenko, R. Becker, W. Grünert, *Appl. Catal. B: Environ.* 182 (2016) 213–219.
- [19] B.M. Weiss, K.B. Caldwell, E. Iglesia, *J. Phys. Chem. C* 115 (2011) 6561–6570.
- [20] A.Y. Stakheev, A.I. Mytareva, D.A. Bokarev, G.N. Baeva, D.S. Krivoruchenko, A.L. Kustov, M. Grill, J.R. Thøgersen, *Catal. Today* 258 (2015) 183–189.
- [21] I. Ellmers, R. Pérez Vélez, U. Bentrup, W. Schwieger, A. Brückner, W. Grünert, *Catal. Today* 258 (2015) 337–346.
- [22] A. Boubnov, H.W.P. Carvalho, D.E. Doronkin, T. Günter, E. Gallo, A.J. Atkins, C.R. Jacob, J.-D. Grunwaldt, *J. Am. Chem. Soc.* 136 (2014) 13006–13015.